ACS Infectious Diseases

Article

pubs.acs.org/journal/aidcbc

Molecular Mechanism of Avibactam-Mediated β-Lactamase Inhibition

Dustin T. King,[†] Andrew M. King,[‡] Sarah M. Lal,[‡] Gerard D. Wright,*[,‡] and Natalie C. J. Strynadka*[,†]

[†]The Department of Biochemistry and Molecular Biology and Center for Blood Research, University of British Columbia, 2350 Health Sciences Mall, Vancouver, British Columbia V6T 1Z3, Canada

[‡]M. G. Department of Biochemistry and Biomedical Sciences and the Department of Chemistry, DeGroote Institute for Infectious Disease Research, McMaster University, Hamilton, Ontario L8S 4K1, Canada

Supporting Information

ABSTRACT: Emerging β-lactamase-mediated resistance is threatening the clinical utility of the single most prominent class of antibacterial agents used in medicine, the β-lactams. The diazabicyclooctane avibactam is able to inhibit a wider range of serine β-lactamases than has been previously observed with β-lactamase inhibitors such as the widely prescribed clavulanic acid. However, despite its broad-spectrum activity, variable levels of inhibition have been observed for molecular class D β-lactamases. In order to better understand the molecular basis and spectrum of inhibition by avibactam, we provide structural and mechanistic analysis of the compound in complex with important class A and D serine β-lactamases. Herein, we reveal the 1.7- and 2.0-Å-resolution crystal structures of avibactam covalently bound to class D β-lactamases OXA-10 and OXA-48. Furthermore, a kinetic analysis of key active-site mutants for class A β-lactamase CTX-M-15 allows us to propose a validated mechanism for avibactam-mediated β-lactamase inhibition including a unique role for S130, which acts as a general base. This study provides molecular insights that will aid in the design and development of avibactam-based chemotherapeutic agents effective against emerging drug-resistant microorganisms.

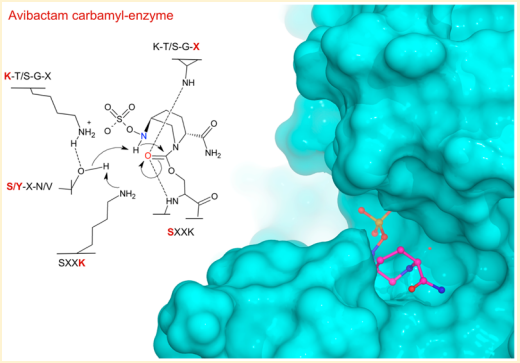

KEYWORDS: β-Lactamase, avibactam, inhibition

The β-lactam antibiotics target the final synthesis step in peptidoglycan (PG) biogenesis, whereby they act as substrate analogues of the penultimate D-ala-D-ala on the PG stem peptide to inhibit the penicillin binding protein (PBP)-catalyzed transpeptidation of adjacent PG strands. The most clinically prevalent resistance mechanism for the β-lactams in Gram-negative bacteria is the expression of β-lactamase enzymes that hydrolyze the four-membered lactam ring, yielding an inactivated product. These enzymes are often encoded on readily transferable plasmids that facilitate their transmission throughout microbial populations.[1]

The β-lactamases are often grouped into four distinct classes (A-D) based upon sequence homology.[2] The class A, C, and D serine β-lactamases (SBLs) evolved from the PBP transpeptidases and are the most clinically prevalent and employ an active-site serine as a nucleophile in β-lactam hydrolysis. In contrast, the class B metallo-β-lactamases (MBLs) utilize active-site zinc ions to mediate lactam bond fission. SBL-catalyzed β-lactam hydrolysis occurs via the formation and subsequent hydrolysis of a serine-bound acyl enzyme intermediate. Despite having a low overall sequence identity, amino acid sequence comparisons and structural analysis have identified three common active-site motifs among the SBLs: motif (i) harbors the nucleophilic serine required for acylation (SXXK), motif (ii) is required for protonation of the β-lactam nitrogen leaving group upon acylation (S/Y-X-N/V), and motif (iii) is involved in activation of the motif ii S/Y proton donor and in substrate recognition and oxyanion stabilization (K/R-T/S-G).[2] The class A enzymes have a conserved E166 (thought to be the general base required for activation of the catalytic water during hydrolytic deacylation), located in a region known as the Ω loop (residues 161−179). In contrast, the class D (OXA) enzymes lack Ω loop E166 and instead involve a carboxylated lysine (i.e., lysine reversibly modified with CO_2 at the ε amino group) in a SXXK motif, which is thought to play a dual role as the general base involved in both serine activation during acylation and in activation of the catalytic water during hydrolytic deacylation.[3−5]

To overcome SBL-mediated resistance, three β-lactam-based inhibitors were introduced into clinical practice in the late 1970s and early 1980s: clavulanic acid, sulbactam, and tazobactam.[6] These compounds are mechanism-based covalent inactivators that form a stable acyl-enzyme intermediate with the catalytic serine. At clinically used concentrations, the bound inhibitor hydrolytically deacylates, either directly or through a series of covalent intermediates, resulting in the eventual turnover of inactivated inhibitor and catalytically active

Received: January 15, 2015
Published: January 22, 2015

DOI: 10.1021/acsinfecdis.5b00007
ACS Infect. Dis. 2015, 1, 175−184

enzyme.[7] Traditionally, these inhibitors target the class A β-lactamases and are clinically ineffective against strains harboring the emerging class C and D SBL enzymes.[8] Furthermore, there are now several class A β-lactamases that have evolved resistance to these compounds (e.g., inhibitor-resistant TEM and complex mutant TEM),[6,9] making the development of novel inhibitors paramount.

Perhaps of greatest promise for the immediate future are the novel class of non-β-lactam-based β-lactamase inhibitors termed diazobicyclooctanes (DBOs). These were originally designed in the late 1990s and display remarkably potent and broad-spectrum inhibition of SBLs. The DBO compound avibactam is currently in phase III clinical development as part of a combination therapy in conjunction with ceftazidime to treat complicated urinary-tract and intra-abdominal infections.[10] Ceftazidime-avibactam is active against the majority of Enterobacteriaceae, including multidrug resistant strains and importantly is effective against *Pseudomonas aeruginosa*.[11] In animal models, avibactam-ceftazidime has been utilized to effectively treat ceftazidime-resistant Gram-negative bacterial septicemia, meningitis, pneumonia, and pyelonephritis. The avibactam-ceftazidime safety and tolerability in clinical trials have been outstanding, and there have been relatively few adverse drug affects documented.[11]

Although avibactam displays excellent inhibitory activity against the class A and C enzymes, more variable levels of inhibition have been observed toward the class D SBLs.[12] Avibactam forms a unique carbamyl linkage with the catalytic serine, which does not decompose via a hydrolytic mechanism as is true for the β-lactam-based SBL inhibitors (Figure 1).

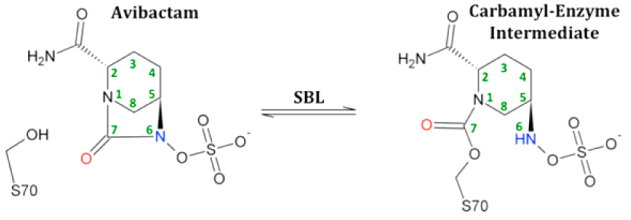

Figure 1. Avibactam-mediated reversible SBL inhibition.

Instead, the decarbamylation of avibactam occurs via recyclization of the DBO fused-ring structure, reforming the intact inhibitor that can then either recarbamylate the same active site or be released into solution to inactivate subsequent SBLs.[13] The most common mechanism of resistance to ceftazidime-avibactam is the expression of β-lactamases that are unhindered by avibactam (e.g., the MBLs and the majority of class D SBLs). Crystal structures of avibactam bound to class A enzymes BlaC and CTX-M-15 and class C enzyme AmpC have recently been released.[14,15] Additionally, Lahiri and colleagues recently reported the crystal structures of OXA-24 and OXA-48 bound to avibactam at 2.3 and 2.4 Å resolution.[16] However, the mechanism and roles of individual amino acids in SBLs that contribute to avibactam activity remain largely unresolved.

To address the underlying molecular details of avibactam inhibition, we have undertaken a multifaceted structural, kinetic, and mutagenesis study on known targets. We have utilized class A enzyme CTX-M-15, which is the most widely distributed extended-spectrum β-lactamase (ESBL) globally[17] as a model enzyme. The universally conserved S130 acts both as a general acid during carbamylation and a general base during decarbamylation in the avibactam recycling pathway. We further reveal the 2.0- and 1.7-Å-resolution crystal structures of avibactam covalently bound to the catalytic serine of the clinical variants, OXA-48 and OXA-10. Narrow-spectrum oxacillinase OXA-10 is among the most prevalent class D enzymes in *P. aeruginosa*,[18] and carbapenem hydrolyzing OXA-48 is prevalent in the emerging carbapenem-resistant Enterobacteriaceae (CRE).[12,19] The data elucidates the active-site features likely responsible for the variable inhibition observed for this class of SBL enzymes that uniquely relies on a post-translationally modified (carboxylated) lysine during catalysis.

RESULTS AND DISCUSSION

Inhibition of CTX-M-15 by Avibactam. We have solved the cocrystal structure of avibactam complexed with the CTX-M-15 class A SBL in space group $P2_1$ at 1.6 Å resolution, with two protein chains in the asymmetric unit (ASU). [See Table S1 in the Supporting Information (SI) for a full list of data collection and refinement statistics.] Recently, Docquier et al.

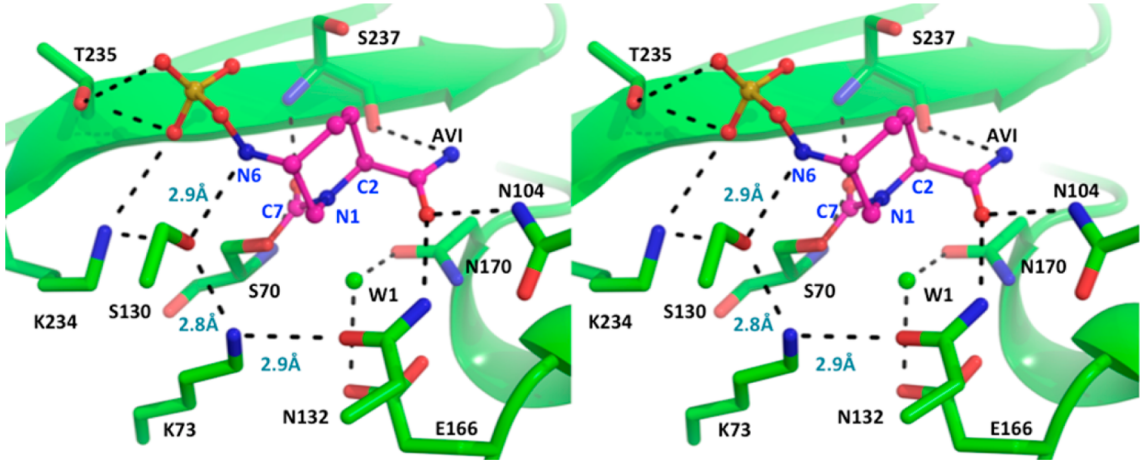

Figure 2. Inhibition of CTX-M-15 by avibactam. Stereoview active-site close-up of carbamyl-avibactam-bound CTX-M-15. The carbon atoms of avibactam are pink, and all other atoms are colored by type (N, blue; O, red; S, yellow). The avibactam-bound CTX-M-15 protein backbone is displayed as a green cartoon. The catalytic water (W1) is shown as a green sphere. Hydrogen bonding and electrostatic interactions are depicted as black dashes.

DOI: 10.1021/acsinfecdis.5b00007
ACS Infect. Dis. 2015, 1, 175−184

Table 1. Kinetic Values for the Carbamylation and Decarbamylation of Avibactam against a Panel of CTX-M-15 Active-Site Mutants[a]

parameter	WT	K73A	N104A	S130A	N132A	E166Q	K234A
on-rate k_2/K_i (M^{-1} s^{-1})	$1.6 \pm 0.2 \times 10^5$	$2.8 \pm 0.1 \times 10^{-1}$	$3.9 \pm 0.2 \times 10^4$	3.3 ± 0.4	$3.7 \pm 0.3 \times 10^5$	$9.3 \pm 1.2 \times 10^4$	$8.0 \pm 0.9 \times 10^2$
off-rate k_{off} (s^{-1})	$1.5 \pm 0.1 \times 10^{-4}$	$2.1 \pm 0.3 \times 10^{-7}$	$7.1 \pm 0.1 \times 10^{-5}$	$7.7 \pm 0.7 \times 10^{-7}$	$1.6 \pm 0.1 \times 10^{-4}$	$1.8 \pm 0.3 \times 10^{-4}$	$4.0 \pm 0.8 \times 10^{-5}$
off-rate $t_{1/2}$ (min)	76	6×10^4	160	9×10^3	74	63	292
K_d (μM)	0.001	0.8	0.002	0.2	0.001	0.002	0.05

[a]The carbamylation and decarbamylation rates were measured using colorimetric reporter substrate nitrocefin. The K_D values are calculated from the carbamylation and decarbamylation rates.

presented a 1.1-Å-resolution X-ray cocrystal structure of the avibactam-CTX-M-15 carbamyl-enzyme complex, which crystallized in space-group $P2_12_12_1$ with a single protein monomer in the ASU (PDB ID 4HBU). However, a close electrostatic interaction between the bound avibactam sulfate group and R42 on an adjacent monomer was observed as a crystallographic artifact (avibactam N6 sulfate to R42 guanidino $\eta1$ distance = 3.0 Å).[14] Despite this difference in avibactam binding, we find that the compound itself takes on a nearly identical conformation between the two crystal forms and resulting structures (Figure S1a in the SI).

From our cocrystal structure, we see that upon carbamylation by the SXXK S70, the avibactam C7−N6 amide bond is liberated rather than the C7−N1 bond (Figure 2). The avibactam sulfate projects into an electropositive pocket formed by K234 and is stabilized by interactions with T235 and K234 on motif iii. The R1 carboxamide is oriented away from the active-site core and is within hydrogen bonding distance (3.0 and 2.7 Å) away from the side-chain amide nitrogens of N104 and N132 (Figures 2 and S1).

Water (W1), the nucleophile responsible for hydrolytic deacylation of the β-lactams, occupies the typical catalytic position, oriented by hydrogen bonds to the side chains of E166 and N170 protruding from the CTX-M-15 Ω-loop motif. We suggest that a major contributing factor to the avoidance of the carbamyl enzyme to hydrolytic decarbamylation is that the carbamyl carbon is less susceptible to nucleophilic attack than its ester (acyl-enzyme) counterpart.[20,21] This stability is presumably due to a resonance effect in which the lone pair of electrons on the sp^2-hybridized N1 aligns with the carbonyl C═O p orbitals, thereby increasing the electron density at the electrophilic carbonyl carbon.[22] Carbamyl bond formation is a common feature observed for inhibitors of serine hydrolases, some of which have also been shown to retain the catalytic water in the carbamylated state.[23,21]

Carbamylation/Decarbamylation Kinetics for CTX-M-15 Active-Site Mutants. To evaluate the mechanistic details governing the reversible recyclization reaction of avibactam inhibition, we mutagenized key active-site residues within CTX-M-15 and measured enzyme activity using the colorimetric cephalosporin, nitrocefin, as a reporter substrate. We confirmed that mutants adopt a WT fold by dynamic light scattering and that no hydrolysis of avibactam occurred using liquid chromatography−mass spectrometry (LC−MS) (Figures S3 and S7−S16).[12]

For class A SBLs such as CTX-M-15, there are alternative views on the mechanism of S70 activation during β-lactam acylation. In one perspective, Ω-loop E166 activates S70 for nucleophilic attack by O-γ deprotonation through a water molecule. The second proposal involves K73 as the base responsible for S70 activation. Here, we find that E166Q has a comparable avibactam carbamylation rate to wild type [WT and E166Q carbamylation rates (k_2/K_i) = $1.6 \pm 0.2 \times 10^5$ and $9.3 \pm 1.2 \times 10^4$ M^{-1} s^{-1}], suggesting that E166 is not directly involved in the carbamylation mechanism. In contrast, K73A was almost completely carbamylation-deficient ($2.8 \pm 0.1 \times 10^{-1}$ M^{-1} s^{-1}) (Table 1). These data support the proposition that K73 is the general base responsible for S70 activation during avibactam carbamylation. This may in part facilitate avibactam's ability to inhibit each SBL subclass that bears the universally conserved SXXK lysine.

During carbamylation, the avibactam N6 nitrogen is protonated following ring opening. We hypothesized that the S130 γ-OH is responsible for this protonation event due to its proximity to N6 in the carbamyl-enzyme crystal structure (2.9 Å, Figure 2). We observed a dramatic reduction in the carbamylation rate for the S130A mutant [WT and S130A carbamylation rates (k_2/K_i) = $1.6 \pm 0.2 \times 10^5$ and 3.3 ± 0.4 M^{-1} s^{-1}] (Table 1). Therefore, we propose that in an analogous fashion to its role in β-lactam nitrogen protonation during acylation, S130 also acts as the general acid responsible for protonation of the avibactam N6 during carbamylation.

For subsequent avibactam recyclization to occur, the N6 nitrogen must be deprotonated to facilitate intramolecular attack of the carbamyl linkage reforming the N6−C7 bond. Because of its proximity to the N6 nitrogen in the CTX-M-15-bound structure (2.9 Å, Figures 2 and S1b), Docquier et al. proposed that S130 may potentially act as the general base responsible for reversible recyclization.[14] To test this, we analyzed the decarbamylation rate for the S130A CTX-M-15 mutant. The carbamyl enzyme intermediate was virtually unable to decarbamylate in the S130A mutant [WT and S130A decarbamylation rates (k_{off}) = $1.5 \pm 0.1 \times 10^{-4}$ and $7.7 \pm 0.7 \times 10^{-7}$ s^{-1}] (Table 1), consistent with the role of S130 as the general base responsible for avibactam recyclization. Despite intensive research on SBLs over the past several decades, this is the first example of S130 acting as a general base, a feature that exemplifies the novelty of the avibactam inhibitor and the functional plasticity of this residue.

In the carbamyl avibactam-CTX-M-15 crystal structure, K73 and K234 are directly hydrogen bonded to the side chain O-γ of S130, suggesting that they may be responsible for regulating the protonation state of S130 during carbamylation/decarbamylation (Figures 2 and S1b). The K73A mutant mimics the effect of S130A whereby it is almost completely deficient in decarbamylation (k_{off} = $2.1 \pm 0.3 \times 10^{-7}$ s^{-1}). However, K234 displays only a moderate reduction in decarbamylation rate as compared to the wild-type enzyme (Table 1). We therefore

DOI: 10.1021/acsinfecdis.5b00007
ACS Infect. Dis. 2015, 1, 175−184

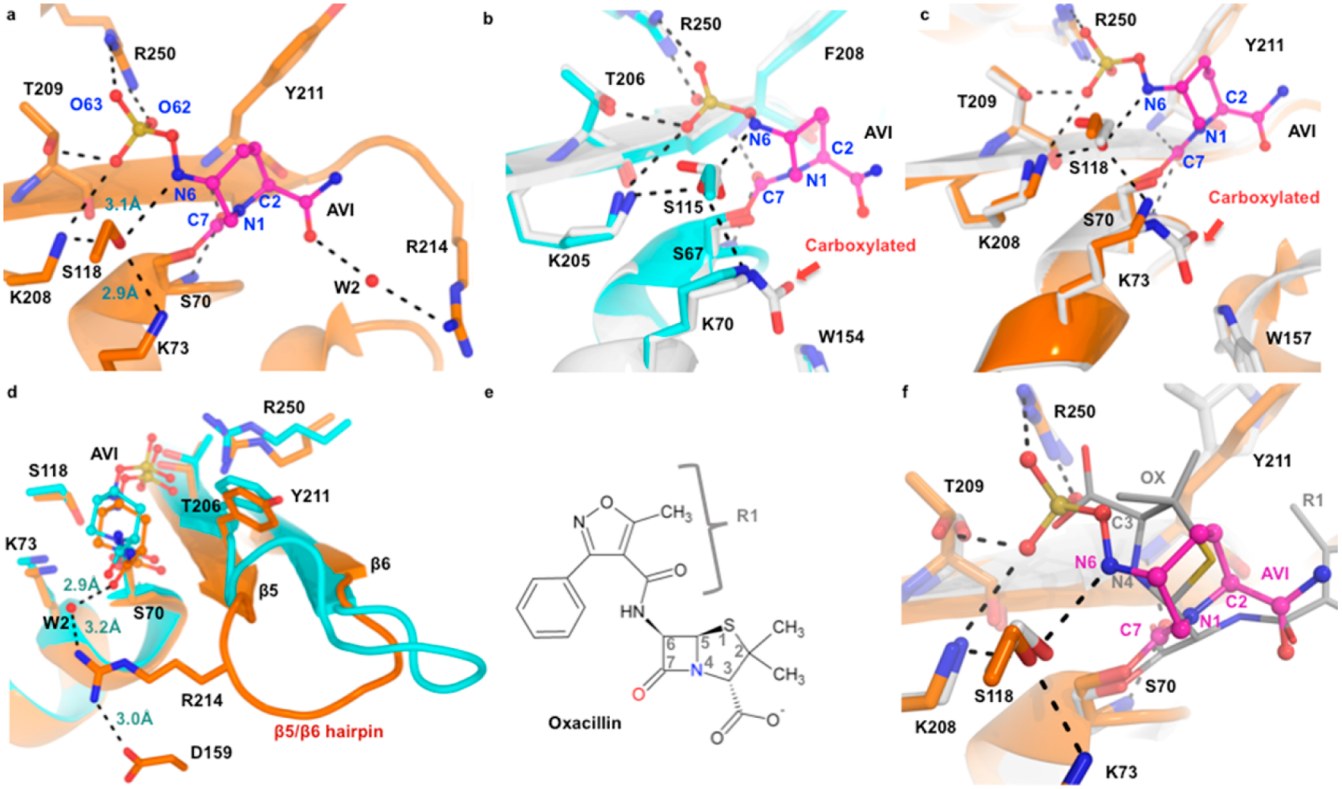

Figure 3. Inhibition of OXA-48 and OXA-10 by avibactam. (a) Active-site close-up of carbamyl-avibactam OXA-48. The carbon atoms of avibactam are pink with all other noncarbon atoms colored by atom type. The avibactam-bound OXA-48 protein chain is displayed in an orange cartoon representation, and key active-site residues are shown as sticks with atoms colored by type. (b) Active-site overlay of carbamyl-avibactam and uncomplexed OXA-10. The avibactam-bound and unbound OXA-10 protein chains are illustrated in a cyan and white cartoon representation, and key active-site residues are depicted as sticks with atoms colored by type (OXA-10 numbering). (c) Active-site overlay of carbamyl-avibactam and uncomplexed OXA-48. The carbamyl-avibactam and OXA-48 protein chain are displayed as in A. The unbound OXA-48 protein chain is illustrated in a gray cartoon representation, and key active-site residues are depicted as sticks with atoms colored by type. (d) Active-site overlay of carbamyl-avibactam OXA-48 and OXA-10. The OXA-48 and OXA-10 protein chains, active-site residues, and bound avibactam are displayed as in a and b. (e) Structure of oxacillin. (f) Active-site overlay of carbamyl-avibactam-bound OXA-48 and acyl-oxacillin-bound K84D OXA-24 (PDB ID 4F94). The carbamyl-avibactam-bound structure is displayed as in a. The OXA-24 protein backbone is illustrated as a white cartoon, and key active-site residues are shown in a stick representation with atoms colored by type. The acyl-oxacillin carbon atoms are gray, and all other atoms are colored by type. In a, b, c, d, and f, all hydrogen bonding and electrostatic interactions are depicted as black dashes.

suggest that K73 may potentially be the base responsible for S130 activation during recyclization, with K234 playing an additional electrostatic role in modulating the pK_a depression of S130 to facilitate its necessary oxyanion state.

The class A SBL-catalyzed hydrolytic deacylation of β-lactams is thought to proceed through E166-catalyzed hydrolysis of the acyl-enzyme intermediate and subsequent protonation of the S70 O-γ via an E166 coordinated water molecule.[24] However, for avibactam recyclization, we find that the E166Q decarbamylation rate is virtually identical to the wild-type rate, suggesting that E166 is not required for S70 protonation (Table 1). Because of the close proximity of the K73 N-ζ to the S70 O-γ in the unbound CTX-M-15 crystal structure (2.7 Å)[14] and the apparent decarbamylation deficiency of the K73A mutant ($t_{1/2} \approx 1000$ h), we suggest that K73 acts as part of a concerted proton shuttle pathway for S70 regeneration during avibactam decarbamylation.

In the carbamyl avibactam-CTX-M-15 crystal structure, the side-chain amide nitrogen atoms of N132 and N104 are within hydrogen bonding distance 2.7 and 3.0 Å away from the avibactam C2 carboxamide oxygen (Figures 2 and S1b). We found that mutant N104A, but not N132A, had a 4-fold reduction in the carbamylation rate as compared to the WT enzyme but a minimal effect on decarbamylation (Table 1). Previous structural and kinetic analysis suggests that the N104 side -chain amide nitrogen is also important for the stabilization of the acylamide R1 group of the β-lactam antibiotics in the class A SBLs.[25,26] Thus, the role of N104 in class A β-lactamases is likely to contribute to Michaelis complex formation by interacting with the avibactam C2 carboxamide in an analogous fashion to the R1 side chain of β-lactams. Future drug design efforts should seek to maintain a hydrogen bond acceptor at the avibactam C2 carboxamide oxygen position.

Inhibition of the Class D SBLs by Avibactam. To understand the structural basis for DBO-mediated inhibition of the class D β-lactamases, we determined cocrystal structures of avibactam bound to OXA-10 and OXA-48 at three different pH values (6.5, 7.5, and 8.5, hereafter called OXA-48-AVI6.5, OXA-48-AVI7.5, and OXA-48-AVI8.5) to 1.7, 2.5, 2.1, and 2.0 Å resolution, respectively (Table S1). Generally, all protein monomers within the ASU contain high structural similarity [with root-mean-square deviations (rmsd's) of <0.2 Å for all common α-carbon (CA) atoms in all chains in the ASU]. Therefore, we limit our analysis to chain A for each product complex. For simplicity, we further limit our analysis to OXA-

DOI: 10.1021/acsinfecdis.5b00007
ACS Infect. Dis. 2015, 1, 175−184

48-AVI7.5 unless otherwise stated. All avibactam-bound complexes display a clear and unambiguous ligand omit map F_o-F_c electron density for avibactam within the active site of each protein chain in the ASU (Figure S2). The carbamyl avibactam molecules were refined at full occupancy, with the exception of the OXA-48-AVI8.5 (chains A and B), which were refined at an occupancy of 0.7 (Table S1).

The high resolution of the models allows us to make detailed observations about key active-site interactions. For clarity, we use OXA-48 residue numbering throughout the text when describing both OXA-48 and OXA-10, except in Figure 3b, whereby we use OXA-10 numbering for consistency with the PDB file. The average temperature factors for the refined avibactam in the OXA-48- and OXA-10-bound structures are 22.4 and 17.5 Å^2 (similar to the average protein B factors of 30.3 and 22.6 Å^2), indicating that the inhibitor is bound in a rigid fashion with little conformational variation and flexibility (Table S1). In the complexes, the bound avibactam forms a carbamyl bond between the active-site S70 O-γ and its C7 carbon, as evidenced by the continuous F_o-F_c ligand omit map electron density in this region (Figure S2). Like the class A and C enzymes (CTX-M-15 and AmpC),[14] the C7−N6 bond breaks rather than the C7−N1 bond upon class D SBL-mediated carbamylation. We attribute the C7−N6 bond fission in part to the fact that N6-OSO3$^-$ is a better leaving group than the corresponding RR′N1$^-$. From a structural standpoint, the location of S118 (equivalent to S130 in the class A enzymes) likely also contributes to the observed bond fission as it is ideally positioned to protonate an N6 rather than an N1 leaving group (Figure 3a,b).

In the OXA-48 and OXA-10 carbamylated forms, the six-membered piperidine ring of avibactam adopts a chair-type conformation, with the C4 and N1 atoms located above and below the plane (Figure 3a,b). The C7 carbonyl oxygen of the newly formed carbamyl linkage is located in the oxyanion hole of the enzyme and is bound by the backbone amide protons of S70 and Y211 at 2.7 and 2.8 Å, respectively. The avibactam sulfate group projects into a positively charged cavity consisting of R250, T209, and K208, which binds the analogous C3/C4 carboxylate of β-lactams (Figures 3a,b and S4).[27] OXA-48 and OXA-10 display a strong electrostatic interaction between the avibactam sulfate oxygens (O62 and O63) and R250 guanidino groups η1 and η2 at 2.8 and 3.2 Å, an interaction that is not observed in the class A and C SBL-avibactam complexes. In the OXA-48- and OXA-10-bound structures, the avibactam C2 carbamate is not stabilized by hydrogen bonding with asparagine residues as observed in the class A and C carbamyl avibactam-bound CTX-M-15 and PAO1 AmpC crystal structures.[14]

When aligning the native and avibactam-bound OXA-10 and OXA-48 crystal structures, we observe that the protein chains are nearly identical (rmsd on all common C_α atoms = 0.4 and 0.4 Å), with a remarkably similar juxtaposition of active-site residues (Figure 3b,c). Thus, the class D SBL active site is poised for interaction with avibactam without the need for complicated conformational rearrangements that can substantially slow acylation, as observed for *S. aureus* PBP2a.[28,29]

Comparison of Carbamyl-Avibactam in Class D SBLs OXA-10 and OXA-48. The OXA-10 and OXA-48 enzymes differ by 2 orders of magnitude in their avibactam carbamylation rates ($1.1 \pm 0.1 \times 10^1$ and $1.4 \pm 0.1 \times 10^3$ M^{-1} s^{-1}), despite having a virtually identical arrangement of catalytic residues (Figure 3d).[12] Although the carboxylation of K73 may be important to the observed carbamylation rates (see discussion below), structural differences between enzymes may also play a role. When overlaying the avibactam-bound OXA-48 and OXA-10 crystal structures (49% amino acid sequence identity), we see that the two protein chains align very well (rmsd on 112 common CA atoms = 0.97 Å). The only substantial difference between the two proteins is a β-hairpin connecting strands β5 and β6 (Figure 3d), which flanks the active site and is an important feature defining carbapenemase activity via interaction with the carbapenem hydroxyethyl moiety.[30] For OXA-48, β-hairpin residue R214 interacts electrostatically with D159 on the Ω loop (R214 η1 to D159 δO distance = 3.0 Å), bringing the β-hairpin closer to the catalytic core than observed for the elongated OXA-10 β5-β6 hairpin (Figure 3d). From the OXA-48-bound avibactam structure in two out of four monomers in the ASU, we see that there is a hydrogen bond between the R214 η2 guanidino nitrogen and a water molecule (W2, refined at full occupancy) at 2.9 Å, which in turn hydrogen bonds to the amide nitrogen of the avibactam C2 carboxamide at 3.0 Å (Figure 3d). Therefore, the β5-β6 hairpin may be important for stabilizing the avibactam C2 carboxamide, and thus future structure-based drug-designed efforts should aim to maintain this water-mediated interaction.

Comparison of Avibactam and β-Lactam Binding in the Class D SBLs. When overlaying avibactam-bound OXA-48 onto the 2.4-Å-resolution crystal structure of acyl-oxacillin-bound K84D OXA-24 (PDB ID 4F94, unpublished data), we see that the two protein chains align well (rmsd = 1.1 Å on 80 common CA atoms). Furthermore, the oxacillin and avibactam ligands display analogous overall orientations despite their chemical differences (Figure 3f). In both structures, the acyl/carbamyl carbonyl oxygen interacts with the backbone amides of oxyanion hole residues S70 and Y211 on strand β5 (OXA-48 residue numbering). The electronegative substituent (the avibactam N6 sulfate and penicillin C3 carboxylate) both project toward the basic patch defined by R250, K208, and T209. Additionally, the avibactam C2 carboxamide and the analogous β-lactam R1 functional group orient away from the catalytic core, toward bulk solvent in both structures (Figure 3f). Taken together, the observed similarities between DBO and β-lactam binding in part help to explain the broad-spectrum SBL target profile for avibactam, which clearly acts as a substrate analogue. The DBO C2 carboxamide group may be a key site for chemical modification in future drug design efforts, as has been the case for the β-lactam R1 moiety.[31]

β-Lactams hydrolytically deacylate from the SBL catalytic serine rather than recyclize to the active antibiotic.[32] However, both the avibactam N6 and the analogous oxacillin N4 atoms are within hydrogen bonding distance (3.1 and 3.3 Å) of recyclization general base S118 (Figure 3f). We propose that recyclization is prohibited in the β-lactams due to an intrinsically high energy barrier to cyclizing the strained four-membered lactam ring, as opposed to that for the five-membered ring that is formed upon avibactam recyclization.

Carboxylation State of Lysine 73 in the Avibactam Carbamyl-Enzyme Complexes. The N-carboxylation state of K73 is sensitive to pH, with carboxylation increasing at higher pH values presumably due to an increased reactivity of K73 to carbon dioxide in more basic solutions and the greater stability of carbamic acid in the anionic form at higher pH.[4] OXA-48 with no avibactam present was crystallized at pH 7.5 and displays a clear, unambiguous K73 omit map F_o-F_c

DOI: 10.1021/acsinfecdis.5b00007
ACS Infect. Dis. 2015, 1, 175−184

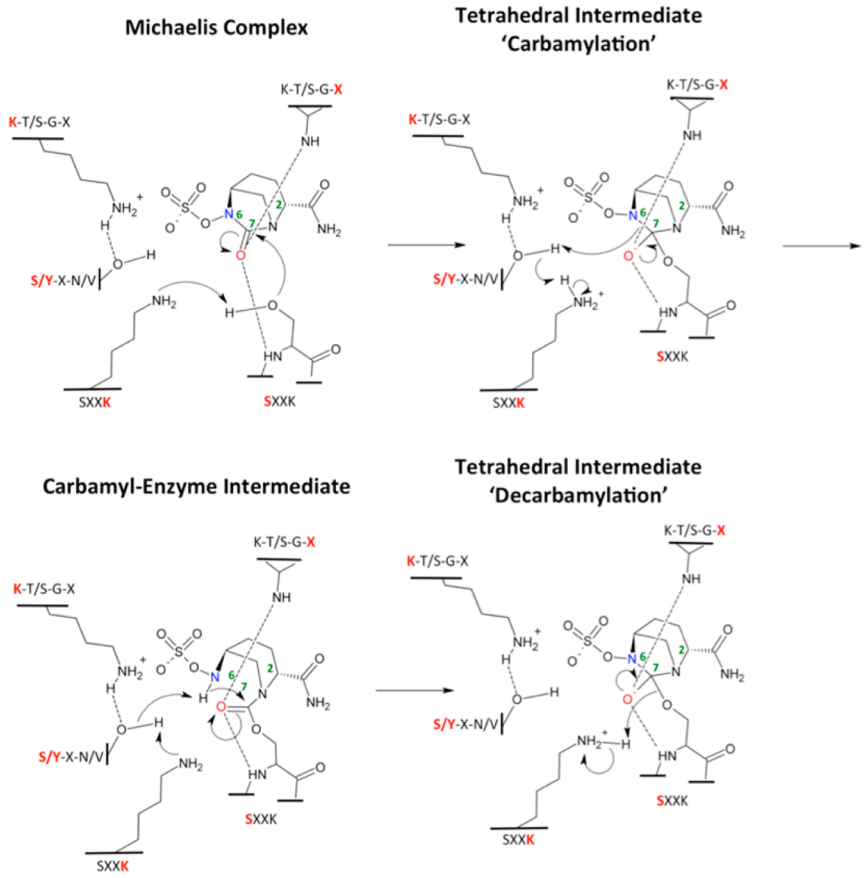

Figure 4. Proposed general catalytic mechanism for avibactam-mediated SBL inhibition.

electron density for carboxylated lysine, which was refined at full occupancy for both monomers within the ASU (Figure S5a). Interestingly, in the avibactam-bound OXA-48 structures at both pH 6.5 and 7.5, no monomers display evidence of carboxylation at K73 upon inspection of the F_o-F_c K73 omit electron density maps (Figure S5b,c). Therefore, the presence of the bound avibactam appears to disfavor K73 carboxylation in the carbamyl-enzyme complexes.

Only in the pH 8.5 structure, OXA-48-AVI8.5, do two out of four monomers in the ASU (chains A and B) display partial occupancy for N-carboxylated K73 (Figure S5d). At the same time, these are the only chains from all OXA-48 structures that display partial rather than full occupancy for avibactam (Table S1). However, it should be noted that at pH 8.5 avibactam was shown to degrade when free in solution by LC−MS (Figure S16), providing an alternative or additional reason for the observed partial occupancy. As an interesting aside, to our knowledge, this is the first report showing that avibactam is not stable at high pH.

Recently, Ehmann et al. have shown by monitoring OXA-10 carbamyl exchange with TEM-1 that OXA-10, like the majority of SBLs tested, undergoes a reversible rather than hydrolytic route to avibactam decarbamylation.[12] Taken together, the absence of K73 N-carboxylation clearly disfavors hydrolytic decarbamylation of avibactam for the class D enzymes. The acyl enzyme crystal structure of OXA-24 bound to tazobactam (which undergoes hydrolytic deacylation rather than decarbamylation) displays a carboxylated K73 (PDB ID 3ZNT, unpublished), further corroborating the notion that motif i lysine carboxylation is a key feature governing hydrolysis in the class D enzymes. However, it is currently unclear whether carboxylated K73 is the general base responsible for S70 activation during carbamylation and how this modification affects avibactam carbamylation rates for the class D SBLs.

In the avibactam-bound OXA-48 structure, the decarboxylated K73 is oriented toward S118 rather than W57 as observed in the unbound, carboxylated state (Figure 3c). In the avibactam-bound form, the decarboxylated K73 hydrogen bonds to S118 at a distance of 2.9 Å, which in turn hydrogen bonds to the N6 proton on avibactam at 3.1 Å (Figure 3a,c). This conformational switch is reminiscent of the CTX-M-15 avibactam-bound structure whereby K73 is hydrogen bonded to S130 (equivalent to the OXA-48 S118) (Figure 2), yet this interaction is not present in the unbound CTX-M-15 structure.[14] We propose that upon avibactam recyclization this hydrogen bonding network results in K73-mediated deprotonation of S118, which in turn removes the avibactam N6 hydrogen facilitating an attack on the carbamyl bond and subsequent recyclization.

Universal Mechanism for Avibactam-Mediated SBL Inhibition. Analysis of the avibactam-bound carbamyl enzyme crystal structures of the class A, C, and D β-lactamases (CTX-M-15, *P. aeruginosa* PA01 AmpC,[14] and OXA-48) reveals that the DBO core takes on a similar orientation with respect to the conserved SBL active-site motifs in all three structures (Figure S6). Taken together, these crystal structures along with the CTX-M-15 mutant kinetic data allows us to propose a universal mechanism for SBL inhibition. Electrostatic stabilization of the N6 sulfate likely helps to orient the bound avibactam in the precatalytic Michaelis complex, whereby the sulfate occupies

DOI: 10.1021/acsinfecdis.5b00007
ACS Infect. Dis. 2015, 1, 175−184

the electropositive pocket formed by SBL motif iii. The catalytic serine is activated via general base-mediated deprotonation (SXXK, Figure 4), likely by K73 for the class A SBLs, K67 for the class C SBLs, and K73 for the class D enzymes. The subsequent attack of the activated serine O-γ on the avibactam C7 carbonyl results in the formation of a transient tetrahedral intermediate that is stabilized by the oxyanion hole of the enzyme (consisting of the backbone amides of the catalytic serine and residue X from the K-T/S-G-X motif (iii)). The lone pair of electrons on the C7 oxygen drive back into carbonyl formation, expelling the negatively charged N6 nitrogen, which is concomitantly protonated by the motif ii serine (or tyrosine for the class C enzymes), resulting in the formation of a stable carbamyl enzyme complex. The complex resists decomposition by hydrolysis likely due in part to the inherent stability of the carbamyl bond and/or by removal of the general base involved in β-lactam hydrolytic deacylation (as proposed for the decarboxylation of the SXXK carboxy-lysine in the class D enzymes). Upon eventual avibactam decarbamylation, a reversible mechanism of recyclization generally occurs, whereby the SXXK lysine takes part in a concerted acid−base shuffling of protons from the motif ii serine (for class A and D) or tyrosine (for class C), which deprotonates the N6 nitrogen facilitating an intramolecular nucleophilic attack on the electrophilic C7 carbamyl carbon. The decarbamylation results in the departure of the catalytic serine leaving group, which likely abstracts a proton from the N-ζ of the now protonated SXXK lysine to regenerate the active site (Figure 4).

Concluding Remarks. Avibactam binds to the three major classes of SBLs (classes A, C, and D) in an overall similar fashion. However, subtle differences in active-site hydrogen bonding networks and electrostatic interactions lead to substantial discrepancies in carbamylation rates both between and within these enzyme subclasses. Using CTX-M-15 as a model enzyme, we show that the motif ii serine is the likely base required for avibactam's characteristic recyclization. The crystal structures of OXA-48 and OXA-10 bound to avibactam uncover unique binding features that should help to guide prospective synthesis efforts targeting the inhibition of the class D SBLs. It is our hope that this study will serve as a valuable tool for the future design and development of this exciting new class of inhibitors.

METHODS

DNA Manipulations and Plasmid Construction. Primers used for PCR DNA amplification and site-directed mutagenesis were purchased from MOBIX lab (McMaster University, Hamilton, ON, Canada) or Integrated DNA Technologies (IDT; Coralville, IA). The list of primer sequences used can be found in Table S2. pET-28b(CTX-M-15), encoding mature CTX-M-15 (Q26-L288), was constructed by amplifying the $bla_{CTX\text{-}M\text{-}15}$ gene from *K. pneumoniae* strain H0142423 (Mt. Sinai Hospital, New York, NY) using CTX-M-15 F and CTX-M-15 R primers and cloning into pET-28b. pET-28b(KPC-2) and pET-28b(OXA-48) were constructed by cloning the mature genes into pET-28b. Genes were synthesized by IDT.

Site-Directed Mutagenesis of CTX-M-15. A two-primer, two-stage PCR method[36] was used to engineer CTX-M-15 variants harboring the following point mutations: K73A, N104A, S130A, N132A, E166Q, and K234A. pET-28b(CTX-M-15) was used as a template in mutagenesis experiments to generate the listed pET-28b(CTX-M-15) variants for protein expression and purification.

Protein Expression and Purification. For kinetics studies, an *E. coli* BL21(DE3) colony transformed with its respective β-lactamase construct, CTX-M-15 (WT, K73A, N104A, S130A, N132A, E166Q, K234A), KPC-2, or OXA-48, was inoculated into LB medium containing 50 μg/mL kanamycin and grown at 37 °C. Protein expression was induced with 1 mM IPTG at OD_{600} 0.7, and cultures were incubated overnight at 16 °C. Cells were harvested by centrifugation, and cell paste from 1 L of culture expressing β-lactamase was washed with 8 mL of 0.85% NaCl, resuspended in buffer containing 50 mM HEPES pH 7.5, 350 mM NaCl, and 20 mM imidazole, and then lysed by cell disruption at 20 000 psi. Lysate was centrifuged using a Beckman JA 25.50 rotor at 20 000 rpm (48 254*g*) for 45 min at 4 °C. The supernatant was applied to a 5 mL HiTrap Ni-NTA column (GE Lifesciences) at a constant flow rate of 3 mL/min. The column was washed with five column volumes of the same buffer, and step gradients of increasing imidazole were used for washing and elution steps. Fractions containing purified β-lactamase, based on SDS-PAGE, were pooled and dialyzed overnight at 4 °C in buffer containing 50 mM HEPES pH 7.5, 150 mM NaCl, and 20% glycerol. All purified enzymes were verified to be >95% pure as assessed by SDS-PAGE and stored at −20 °C.

CTX-M-15 Enzyme Assays. Nitrocefin was synthesized as reported previously.[33] Kinetic parameters of purified mutant CTX-M-15 β-lactamase hydrolysis of nitrocefin were determined at 30 °C in 50 mM HEPES buffer (pH 7.5). Rates of hydrolysis were measured in a 96-well microplate format at 490 nm using a Spectramax reader (Molecular Dynamics). Enzyme concentrations were adjusted so as to yield the following concentrations in 200 μL: WT (0.5 nM), K73A (5 nM), N104A (0.1 nM), S130A (0.1 nM), N132A (0.5 nM), E166Q (100 nM), and K234A (20 nM). All enzyme dilutions were done in 100 ng/μL bovine serum albumin (BSA). Nitrocefin concentrations ranged from 320 to 2.5 μM.

For WT, N104A, and N132A, carbamylation experiments were carried out using a Bio-Logic SFM-4 stopped-flow/quench-flow instrument using a cuvette with a 2 mm path length. A four-syringe method was used to give a constant final concentration of 20 nM enzyme and 200 μM nitrocefin in 50 mM HEPES pH 7.5 with 0.01% Tween20. The maximum concentration of avibactam used was 10 μM. The total flow rate was adjusted to 3 mL/s. Absorbance was read continuously at 490 nm. For data analysis, the offset between reaction initiation and the first absorbance read was 700 ms. For E166Q and K234A, acylation experiments were carried out in a 96-well microplate format monitored continuously at 490 nm using a Spectramax reader (Molecular Dynamics). Enzyme concentrations were adjusted so as to yield the following final concentrations in 200 μL wells: 200 nM E166Q and 10 nM K234A. For E166Q on-rate assays, the maximum concentration of avibactam used was 1 μM with 100 μM nitrocefin as the reporter substrate. For K234A on-rate assays, the maximum concentration of avibactam used was 256 μM with 200 μM nitrocefin as the reporter substrate.

Data were fit to a two-step reversible inhibition model as described previously,[34]

$$\mathrm{E} + \mathrm{I} \underset{k_{-1}}{\overset{k_1}{\rightleftharpoons}} \mathrm{EI} \underset{k_{-2}}{\overset{k_2}{\rightleftharpoons}} \mathrm{EI}^* \qquad (1)$$

where

DOI: 10.1021/acsinfecdis.5b00007
ACS Infect. Dis. 2015, 1, 175−184

$$K_i = \frac{k_{-1}}{k_1} \quad (2)$$

and

$$K_i^* = \frac{K_i k_{-2}}{k_2 + k_{-2}} \quad (3)$$

Time courses were fit to eq 4 to obtain the pseudo-first-order rate constant for enzyme inactivation, k_{obs}.[35]

$$P = v_s t + (v_0 - v_s)\frac{(1 - e^{-kt})}{k} \quad (4)$$

where P, v_s, v_0, and t are the amount of product formed, the steady-state rate (approximated by a no-enzyme control), the initial rate (approximated by a no-inhibitor control), and time. Equation 5 was used to derive k_2/K_i, the second-order rate constant for enzyme carbamylation,

$$k_{obs} = k_{-2} + \frac{k_2}{K_i}\frac{[I]}{\left(1 + \frac{[S]}{K_m}\right)} \quad (5)$$

where [I], [S], and K_m are the concentrations of avibactam and nitrocefin and the K_m value of each enzyme for nitrocefin (Table S3). Error values reported are the standard errors of the fit.

For K73A and S130A on-rate assays, discontinuous sampling was employed from samples incubated at 30 °C for 120 and 20 h, respectively. Enzyme concentrations were adjusted so as to yield 5 nM K73A and 0.5 nM S130A final. The maximum concentrations of avibactam used were 320 and 64 μM for K73A and S130A, respectively. Rates were measured periodically as above by adding 180 μL of the above to 20 μL of nitrocefin (final concentration 50 μM) and fit to eq 6 to obtain the pseudo-first-order rate constant for enzyme inactivation, k_{obs},[35]

$$v = v_s + (v_0 - v_s)*e^{-kt} \quad (6)$$

where v is the rate of sample taken at time t. Equation 5 was used to derive k_2/K_i, the second-order rate constant for enzyme carbamylation as above. Because the samples were incubated in the absence of nitrocefin, the concentration of substrate used in calculations was 0.

For WT, N104A, and N132A, decarbamylation experiments were performed using the jump dilution method.[36] Enzyme (1 μM) was incubated with avibactam (10 μM) for 20 min at 30 °C and diluted 1/400 in buffer, and 20 μL was added to 180 μL of nitrocefin for final concentrations of enzyme (0.25 nM), avibactam (5 nM), and nitrocefin (400 μM). For E166Q and K234A, decarbamylation experiments were performed using a PD-10 desalting column (GE Healthcare) according to the manufacturer's gravity protocol. E166Q (200 nM) or K234A (20 nM) was incubated with avibactam (5 μM) at 30 °C for 0.5 and 2 h, respectively. After desalting via a PD-10 column (1.4-fold dilution), 180 μL was added to 20 μL of nitrocefin (final concentration 400 μM for K234A and 200 μM for E166Q). For WT, N104A, N132A, E166Q, and K234A, experiments were carried out in 96-well microplate format monitored continuously at 490 nm using a Spectramax reader (Molecular Dynamics). Data were fit to eq 4 to obtain k_{off}. In the off-rate experiment, v_s was approximated by a no-inhibitor control and v_0 by a no-enzyme control. Each error value reported is the standard deviation of three technical replicates.

For K73A and S130A, decarbamylation experiments were performed using a PD-10 spin column as above. K73A (5 nM) or S130A (1 nM) was incubated with avibactam (256 and 128 μM, respectively) at 30 °C for 60 h (K73A) or 3 h (S130A). After the removal of excess avibactam via a PD-10 column (1.4-fold dilution), discontinuous sampling of the mixtures was done by taking 90 μL of the above in 10 μL of nitrocefin (final concentration 100 μM). Data were fit to eq 6 to obtain k_{off}.[35] In the off-rate experiment, v_s was approximated by a no-inhibitor control and v_0 by a no-enzyme control. Each error value reported is the standard deviation of three technical replicates.

Crystallization, Data Collection, and Structure Determination. Avibactam-bound CTX-M-15, OXA-10,[37] and OXA-48 crystals were grown using the sitting drop vapor diffusion method at 25 °C. For CTX-M15, drops contained 2 μL of 30 mg/mL CTX-M15 in an equal volume of precipitant (0.2 M ammonium sulfate, 0.1 M MES pH 6.5, 30% PEG 5K MME, 5 mM avibactam). For OXA-10, drops contained 3 μL of 10 mg/mL protein in an equal volume of precipitant (1.8 M $(NH_4)_2SO_4$, 0.1 M MES pH 6.5, 10 mM $CoCl_2$, 2 mM avibactam). For the OXA-48 crystal structures, drops contained 2 μL of 50 mg/mL protein in an equal volume of precipitant [(i) OXA-48-AVI6.5/0.1 M sodium cacodylate pH 6.5, 40% v/v MPD, 5 wt %/v PEG 8K, 2 mM avibactam, (ii) OXA-48-AVI7.5/200 mM tris pH 7.5, 0.1 M ammonium chloride, 40% MPD, 5% PEG 8K, 100 mM NaCl, 2 mM avibactam, (iii) native OXA-48 (the OXA-48-AVI7.5 precipitant minus avibactam), and (iv) and OXA-48-AVI8.5/0.1 M TRIS pH 8.5, 20% ethanol, 2 mM avibactam]. Crystallization mother liquor plus 25% glycerol was used as a cryo-protectant, and the crystals were flash frozen in liquid nitrogen. The CTX-M-15-AVI, OXA-48-AVI7.5, OXA-48-AVI8.5, native OXA-48, and OXA-10-AVI crystals diffracted to 1.6, 2.1, 2.0, 1.7, and 2.0 Å at beamline CMCF-2 at the Canadian Light Source (CLS). The OXA-48-AVI6.5 crystals diffracted to 2.5 Å in our in-house X-ray machine. At the CLS and X-ray home source, data was collected at wavelengths of 1.0 and 1.54 Å at a temperature of 100 K.

Data were processed using iMOSFLM[38] and the CCP4[39] program suite. For cross-validation purposes, a total of 5% of reflections were set aside. The avibactam-bound CTX-M-15, OXA-48, and OXA-10 structures were solved by molecular replacement using the program Phaser,[40] with chain A of the native (CTX-M-14, OXA-48 and OXA-10) crystal structures as starting models [PDB IDs 1YLT,[41] 3HBR,[42] and 1FOF[37]]. Several cycles of manual rebuilding in coot,[43] followed by refinement using REFMAC (CCP4),[39] were carried out. All structures were refined with isotropic B-factors. Water and avibactam were added manually by examination of the F_o-F_c and $2F_o-F_c$ electron density maps. Coordinates and structure factors were deposited in the PDB with accession codes (4S2I, 4S2J, 4S2K, 4S2N, 4S2P, and 4S2O) for CTX-M-15-AVI, OXA-48-AVI6.5, OXA-48-AVI7.5, OXA-48-AVI8.5, native OXA-48, and OXA-10-AVI crystal structures. Figures 2, 3, S1, S2, S5, and S7 were designed using PyMol,[44] and Figures S1 and S4 were created using LIGPLOT+.[45]

■ ASSOCIATED CONTENT

Supporting Information

The following file is available free of charge on the ACS Publications website at DOI: 10.1021/id5b00007.

DOI: 10.1021/acsinfecdis.5b00007
ACS Infect. Dis. 2015, 1, 175−184

Figures for ligand electron density, ligand binding modes and distances, dynamic light scattering for CTX-M-15 variants, and LC-MS analysis of avibactam. Tables regarding primers used, nitrocefin kinetics, and crystallographic data collection and refinement statistics. (PDF)

AUTHOR INFORMATION

Corresponding Authors

*E-mail: wrightge@mcmaster.ca.
*E-mail: ncjs@mail.ubc.ca.

Author Contributions

D.T.K. and A.M.K. contributed equally

Author Contributions

The manuscript was written through the contributions of all authors. All authors have given approval to the final version of the manuscript.

Notes

The authors declare no competing financial interest.

ACKNOWLEDGMENTS

This work was financially supported by the following funding agencies: CIHR, HHMI International Scholar Program, CFI, BCKDF, and the Canada Research Chair Programs (to N.C.J.S.). This research was also funded by a CIHR grant (MT-13536), NSERC grant (237480), and by a Canada Research Chair in Antibiotic Biochemistry (to G.D.W.). We thank beamline personnel of CMCF-2 at the Canadian Light Source synchrotron facility (Saskatoon, SK) for their assistance with data collection. We also thank Dr. Alba Guarné, Monica Pillon, and Jeremy Caron for their assistance with DLS experiments. Correspondence and requests for materials should be addressed to G.D.W. (for correspondence relating to enzyme kinetics, LC−MS, and dynamic light scattering) or N.C.J.S. (for correspondence regarding X-ray crystallography of avibactam β-lactamase complexes).

ABBREVIATIONS

PG, peptidoglycan; PBP, penicillin-binding protein; SBL, serine β-lactamase; MBL, metallo β-lactamase; DBO, diazabicyclooctane; ESBL, extended-spectrum β-lactamase; CRE, carbapenem-resistant Enterobacteriaceae; ASU, asymmetric unit; LC−MS, liquid chromatography−mass spectrometry; WT, wild type; rmsd , root-mean-square deviation; PDB, protein data bank

REFERENCES

(1) Bush, K. (2010) Alarming β-lactamase-mediated resistance in multidrug-resistant Enterobacteriaceae. *Curr. Opin. Microbiol. 13*, 558−564.

(2) Bush, K. (2013) The ABCD's of β-lactamase nomenclature. *J. Infect. Chemother. 19*, 549−559.

(3) Delmas, J., Chen, Y., Prati, F., Robin, F., Shoichet, B. K., and Bonnet, R. (2008) Structure and dynamics of CTX-M enzymes reveal insights into substrate accommodation by extended-spectrum beta-lactamases. *J. Mol. Biol. 375*, 192−201.

(4) Golemi, D., Maveyraud, L., Vakulenko, S., Samama, J. P., and Mobashery, S. (2001) Critical involvement of a carbamylated lysine in catalytic function of class D beta-lactamases. *Proc. Natl. Acad. Sci. U.S.A. 98*, 14280−14285.

(5) Schneider, K. D., Karpen, M. E., Bonomo, R. A., Leonard, D. A., and Powers, R. A. (2009) The 1.4 A crystal structure of the class D beta-lactamase OXA-1 complexed with doripenem. *Biochemistry 48*, 11840−11847.

(6) Drawz, S. M., and Bonomo, R. A. (2010) Three decades of beta-lactamase inhibitors. *Clin Microbiol Rev. 23*, 160−201.

(7) Helfand, M. S., Totir, M. A., Carey, M. P., Hujer, A. M., Bonomo, R. A., and Carey, P. R. (2003) Following the reactions of mechanism-based inhibitors with beta-lactamase by Raman crystallography. *Biochemistry 42*, 13386−13392.

(8) Bebrone, C., Lassaux, P., Vercheval, L., Sohier, J. S., Jehaes, A., Sauvage, E., and Galleni, M. (2010) Current challenges in antimicrobial chemotherapy: focus on ß-lactamase inhibition. *Drugs 70*, 651−679.

(9) Cantón, R., Morosini, M. I., Martín, O., de la Maza, O. M., and de la Pedrosa, E. G. (2008) IRT and CMT beta-lactamases and inhibitor resistance. *Clin Microbiol Infect 14*, 53−62.

(10) Lagacé-Wiens, P., Walkty, A., and Karlowsky, J. A. (2014) Ceftazidime-avibactam: an evidence-based review of its pharmacology and potential use in the treatment of Gram-negative bacterial infections. *Core Evid. 9*, 13−25.

(11) Coleman, K. (2011) Diazabicyclooctanes (DBOs): a potent new class of non-β-lactam β-lactamase inhibitors. *Curr. Opin. Microbiol. 14*, 550−555.

(12) Ehmann, D. E., Jahic, H., Ross, P. L., Gu, R. F., Hu, J., Durand-Réville, T. F., Lahiri, S., Thresher, J., Livchak, S., Gao, N., Palmer, T., Walkup, G. K., and Fisher, S. L. (2013) Kinetics of avibactam inhibition against Class A, C, and D β-lactamases. *J. Biol. Chem. 288*, 27960−27971.

(13) Ehmann, D. E., Jahić, H., Ross, P. L., Gu, R. F., Hu, J., Kern, G., Walkup, G. K., and Fisher, S. L. (2012) Avibactam is a covalent, reversible, non-β-lactam β-lactamase inhibitor. *Proc. Natl. Acad. Sci. U.S.A. 109*, 11663−11668.

(14) Lahiri, S. D., Mangani, S., Durand-Reville, T., Benvenuti, M., De Luca, F., Sanyal, G., and Docquier, J. D. (2013) Structural insight into potent broad-spectrum inhibition with reversible recyclization mechanism: avibactam in complex with CTX-M-15 and Pseudomonas aeruginosa AmpC β-lactamases. *Antimicrob. Agents Chemother. 57*, 2496−2505.

(15) Xu, H., Hazra, S., and Blanchard, J. S. (2012) NXL104 irreversibly inhibits the β-lactamase from Mycobacterium tuberculosis. *Biochemistry 51*, 4551−4557.

(16) Lahiri, S. D., Mangani, S., Jahić, H., Benvenuti, M., Durand-Reville, T. F., De Luca, F., Ehmann, D. E., Rossolini, G. M., Alm, R. A., and Docquier, J. D. (2014) Molecular Basis of Selective Inhibition and Slow Reversibility of Avibactam against Class D Carbapenemases: A Structure-Guided Study of OXA-24 and OXA-48. *ACS Chem. Biol.*, DOI: 10.1021/cb500703p.

(17) Poirel, L., Nordmann, P., Ducroz, S., Boulouis, H. J., Arné, P., and Millemann, Y. (2013) Extended-spectrum β-lactamase CTX-M-15-producing Klebsiella pneumoniae of sequence type ST274 in companion animals. *Antimicrob. Agents Chemother. 57*, 2372−2375.

(18) Antunes, N. T., Lamoureaux, T. L., Toth, M., Stewart, N. K., Frase, H., and Vakulenko, S. B. (2014) Class D β-lactamases: are they all carbapenemases? *Antimicrob. Agents Chemother. 58*, 2119−2125.

(19) Zhang, L., Lü, X., and Zong, Z. (2013) The emergence of blaCTX-M-15-carrying Escherichia coli of ST131 and new sequence types in Western China. *Ann. Clin. Microbiol. Antimicrob. 12*, 35.

(20) Alexander, J. P., and Cravatt, B. F. (2005) Mechanism of carbamate inactivation of FAAH: implications for the design of covalent inhibitors and in vivo functional probes for enzymes. *Chem. Biol. 12*, 1179−1187.

(21) Mileni, M., Kamtekar, S., Wood, D. C., Benson, T. E., Cravatt, B. F., and Stevens, R. C. (2010) Crystal structure of fatty acid amide hydrolase bound to the carbamate inhibitor URB597: discovery of a deacylating water molecule and insight into enzyme inactivation. *J. Mol. Biol. 400*, 743−754.

(22) Pattabiraman, V. R., and Bode, J. W. (2011) Rethinking amide bond synthesis. *Nature 480*, 471−479.

(23) Yang, Q., Li, Y., Dou, D., Gan, X., Mohan, S., Groutas, C. S., Stevenson, L. E., Lai, Z., Alliston, K. R., Zhong, J., Williams, T. D., and Groutas, W. C. (2008) Inhibition of serine proteases by a new class of

DOI: 10.1021/acsinfecdis.5b00007
ACS Infect. Dis. 2015, 1, 175−184

cyclosulfamide-based carbamylating agents. *Arch. Biochem. Biophys. 475*, 115−120.
(24) Lamotte-Brasseur, J., Dive, G., Dideberg, O., Charlier, P., Frère, J. M., and Ghuysen, J. M. (1991) Mechanism of acyl transfer by the class A serine beta-lactamase of Streptomyces albus G. *Biochem. J. 279*, 213−221.
(25) Shimamura, T., Ibuka, A., Fushinobu, S., Wakagi, T., Ishiguro, M., Ishii, Y., and Matsuzawa, H. (2002) Acyl-intermediate structures of the extended-spectrum class A beta-lactamase, Toho-1, in complex with cefotaxime, cephalothin, and benzylpenicillin. *J. Biol. Chem. 277*, 46601−46608.
(26) Pérez-Llarena, F. J., Kerff, F., Abián, O., Mallo, S., Fernández, M. C., Galleni, M., Sancho, J., and Bou, G. (2011) Distant and new mutations in CTX-M-1 beta-lactamase affect cefotaxime hydrolysis. *Antimicrob. Agents Chemother. 55*, 4361−4368.
(27) Yasuyuki, F., Noriaki, O., Masayuki, H., Tetsu, N., Kenji, Y., Ryutaro, S., Atsushi, S., Noriyuki, F., Takahiro, K., Hideaki, F., Atsushi, K., Toshikazu, E., Saburo, N., and Tyuji, H. (2003) Molecular Dynamics Study on Class A β-Lactamase: Hydrogen Bond Network among the Functional Groups of Penicillin G and Side Chains of the Conserved Residues in the Active Site. *J. Phys. Chem. B*, 10274−10283.
(28) Eisenmesser, E. Z., Millet, O., Labeikovsky, W., Korzhnev, D. M., Wolf-Watz, M., Bosco, D. A., Skalicky, J. J., Kay, L. E., and Kern, D. (2005) Intrinsic dynamics of an enzyme underlies catalysis. *Nature 438*, 117−121.
(29) Lim, D., and Strynadka, N. C. (2002) Structural basis for the beta lactam resistance of PBP2a from methicillin-resistant Staphylococcus aureus. *Nat. Struct. Biol. 9*, 870−876.
(30) De Luca, F., Benvenuti, M., Carboni, F., Pozzi, C., Rossolini, G. M., Mangani, S., and Docquier, J. D. (2011) Evolution to carbapenem-hydrolyzing activity in noncarbapenemase class D β-lactamase OXA-10 by rational protein design. *Proc. Natl. Acad. Sci. U.S.A. 108*, 18424−18429.
(31) Chen, Y., Shoichet, B., and Bonnet, R. (2005) Structure, function, and inhibition along the reaction coordinate of CTX-M beta-lactamases. *J. Am. Chem. Soc. 127*, 5423−5434.
(32) Majiduddin, F. K., Materon, I. C., and Palzkill, T. G. (2002) Molecular analysis of beta-lactamase structure and function. *Int. J. Med. Microbiol. 292*, 127−137.
(33) Lee, M., Hesek, D., and Mobashery, S. (2005) A Practical Synthesis of Nitrocefin. *J. Org. Chem. 70*, 367−369.
(34) Ehmann, D. E., Jahic, H., Ross, P. L., Gu, R. F., Hu, J., Durand-Reville, T. F., Lahiri, S., Thresher, J., Livchak, S., Gao, N., Palmer, T., Walkup, G. K., and Fisher, S. L. (2013) Kinetics of avibactam inhibition against Class A, C, and D beta-lactamases. *J. Biol. Chem. 288*, 27960−27971.
(35) Morrison, J. F., and Walsh, C. T. (1988) The behaviour and significance of slow-binding enzyme inhibitors. *Adv. Enzymol. Relat. Areas Mol. Biol. 61*, 201.
(36) Copeland, R. A., Basavapathruni, A., Moyer, M., and Scott, M. P. (2011) Impact of enzyme concentration and residence time on apparent activity recovery in jump dilution analysis. *Anal. Biochem. 416*, 206−210.
(37) Paetzel, M., Danel, F., de Castro, L., Mosimann, S. C., Page, M. G., and Strynadka, N. C. (2000) Crystal structure of the class D beta-lactamase OXA-10. *Nat. Struct. Biol. 7*, 918−925.
(38) Battye, T. G., Kontogiannis, L., Johnson, O., Powell, H. R., and Leslie, A. G. (2011) iMOSFLM: a new graphical interface for diffraction-image processing with MOSFLM. *Acta Crystallogr., D 67*, 271−281.
(39) Winn, M. D., Ballard, C. C., Cowtan, K. D., Dodson, E. J., Emsley, P., Evans, P. R., Keegan, R. M., Krissinel, E. B., Leslie, A. G., McCoy, A., McNicholas, S. J., Murshudov, G. N., Pannu, N. S., Potterton, E. A., Powell, H. R., Read, R. J., Vagin, A., and Wilson, K. S. (2011) Overview of the CCP4 suite and current developments. *Acta Crystallogr., D 67*, 235−242.
(40) McCoy, A. J., Grosse-Kunstleve, R. W., Adams, P. D., Winn, M. D., Storoni, L. C., and Read, R. J. (2007) Phaser crystallographic software. *J. Appl. Crystallogr. 40*, 658−674.
(41) Chen, Y., Delmas, J., Sirot, J., Shoichet, B., and Bonnet, R. (2005) Atomic resolution structures of CTX-M beta-lactamases: extended spectrum activities from increased mobility and decreased stability. *J. Mol. Biol. 348*, 349−362.
(42) Docquier, J. D., Calderone, V., De Luca, F., Benvenuti, M., Giuliani, F., Bellucci, L., Tafi, A., Nordmann, P., Botta, M., Rossolini, G. M., and Mangani, S. (2009) Crystal structure of the OXA-48 beta-lactamase reveals mechanistic diversity among class D carbapenemases. *Chem. Biol. 16*, 540−547.
(43) Emsley, P., Lohkamp, B., Scott, W. G., and Cowtan, K. (2010) Features and development of Coot. *Acta Crystallogr., D 66*, 486−501.
(44) Schrödinger, L. *The PyMOL Molecular Graphics System*, Version 1.5.0.4.
(45) Laskowski, R. A., and Swindells, M. B. (2011) LigPlot+: multiple ligand-protein interaction diagrams for drug discovery. *J. Chem. Inf Model. 51*, 2778−2786.

DOI: 10.1021/acsinfecdis.5b00007
ACS Infect. Dis. 2015, 1, 175−184